Session 5
VMSG
Norwich
5-7 January 2015

Bubble, bubble, toil and trouble: The degassing of Katla 1918, a subglacial basaltic eruption

By Jacqueline Owen, Hugh Tuffen, Becky Coats

j.owen2@lancaster.ac.uk
@jacquelineowen

Why study Katla?

Katla is one of Iceland's most dangerous volcanoes. Eruptions tend to be very explosive but also occur relatively frequently (on average twice per century[1]). However, Katla has not erupted since 1918. This is now the longest gap between eruptions since historical records began[2]. This coupled with recent unrest[3], probably triggered by the recent eruption of Katla's neighbour, Eyjafjallajökull in 2010, might mean that an eruption at Katla is imminent.

Figure 1: The Mýrdalsjökull glacier overlying Katla. From this drains the Múlakvísl river which has cut through the 1918 jökulhlaup deposits.

Predicting the behaviour of the next Katla eruption

Katla is a large, predominantly basaltic edifice that lies underneath the Mýrdalsjökull glacier in south Iceland (Figs. 1,2). Although in the past Katla has produced rhyolite (e.g. the 7.5 ka eruption) and fissure eruptions that have extended out under the glacier (e.g. the 934–40 A.D. Eldgjá eruption), the past ~750 years of Katla activity have been dominated by large explosive subglacial basaltic eruptions, that produce vast quantities of tephra and powerful jökulhlaups (glacial floods)[4]. Based on this eruptive history, if Katla does erupt again in the near future, the most likely scenario will be another large explosive subglacial basaltic eruption.

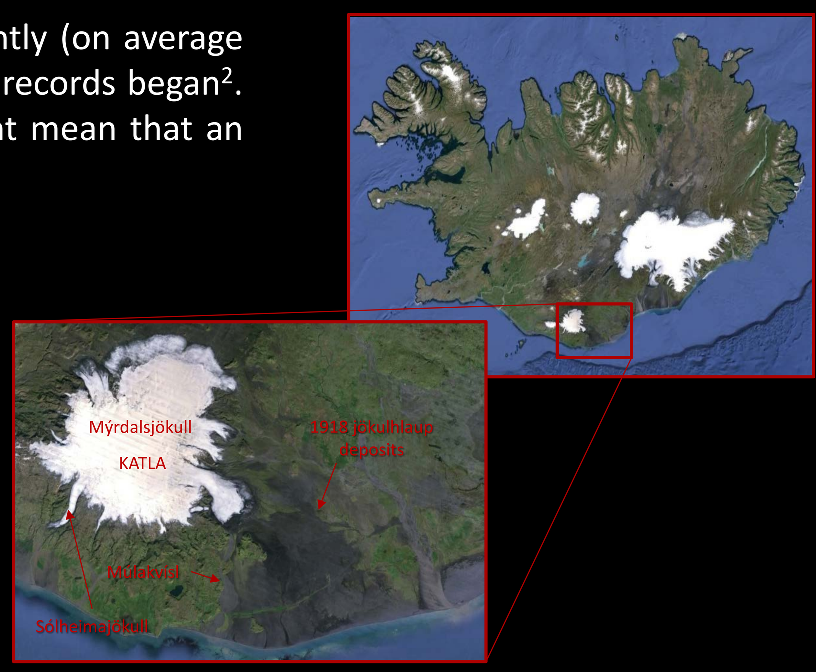

Figure 2: A map showing the location of Katla volcano (residing under the Mýrdalsjökull glacier) in South Iceland.

Project aim

We will conduct a forensic study of the 1918 deposits to reconstruct eruption dynamics. Recent studies have provided evidence that some subglacial eruptions (e.g. the intermediate 2010 Eyjafjallajökull eruption[5] and the 70 ka rhyolitic eruption at Torfajökull[6]) may have been driven by volcanic gasses rather than ice interaction. Is the same true for the basaltic 1918 eruption of Katla? There is also evidence that rapid depressurisation may trigger explosive activity (e.g. Gjálp 1996[7] and the 70 ka Dalakvísl eruption[8]). By examining the fragmentation mechanism and syn-eruptive pressure changes of the 1918 eruption, we hope to gain understanding of what controlled explosivity during the 1918 eruption of Katla which we hope will then help to mitigate the hazards relating to the next Katla eruption.

Sampling jökulhlaup deposits

Melting of ice during the 1918 eruption triggered one of the worlds greatest historic floods[9]. > 8km³ of meltwater was generated[10], flooding an area of 600-800 km² [11], with a discharge rate of >300,000 m³ s⁻¹ [10]. The meltwater also transported icebergs (Fig. 3), giant boulders (Fig. 4), and a huge amount of tephra from the eruption, extending the coastline by 3 km[10]. The jökulhlaup deposits (Fig. 1) are still visible in satellite images today (Fig. 2). We collected four samples from different units[12] of the jökulhlaup deposit, in a vertical profile (Fig. 5) that was exposed by the Múlakvísl river (Figs. 1,2).

Figure 6: The Katla 1918 eruption.

Figure 7: Sólheimajökull glacier looking NW with the pro-glacial lake on the left and Mýrdalsjökull glacier beyond the horizon to the right. The black stripe on the glacier is tephra from the 1918 Katla eruption.

Figure 3: an iceberg dislodged during the 1918 flood.

Figure 4: a ~1400 tonne boulder that was carried > 15 km by the 1918 flood[13].

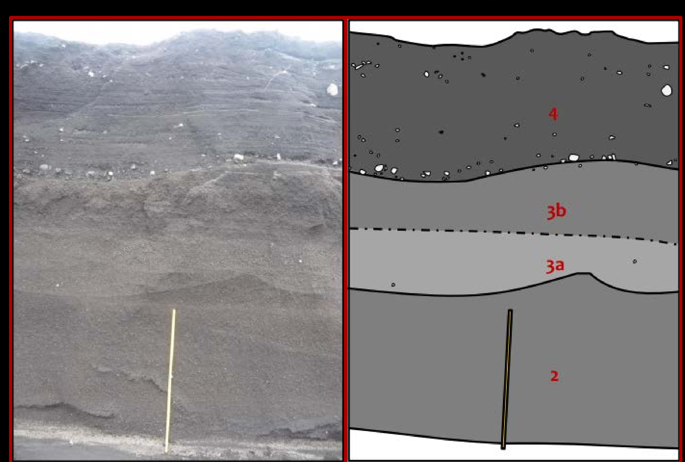

Figure 5: a cross section through the jökulhlaup deposit depicting the 4 units sampled.

Analytical procedures

All samples were dried, then sieved. From the 8000-16000 µm clast size, some representative clasts were chosen and dissected. Half of each clast was retained for Thermogravimetric Analysis (TGA), Fourier Transform Infrared (FTIR) and hotstage experiments. The other half was thin sectioned. Thin sections were also made of representative clasts from the 2000-4000 µm, 250-500 µm and <63 µm clast sizes.

Sampling air-fall tephra

Within two hours of the eruption start, a chimney had been melted through the glacier allowing tephra to also be ejected into the atmosphere[10] (Fig. 6). An eruption column 14 km high was produced, depositing ash over half of Iceland[14]. Air-fall tephra is best preserved on the Mýrdalsjökull glacier. We collected various samples from the Sólheimajökull glacier tongue (Figs. 2,7), including a profile where six discrete layers could be observed (Fig. 8).

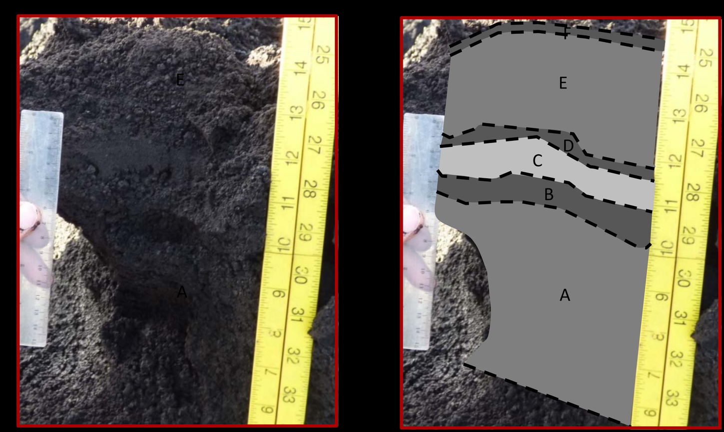

Figure 8: A cross section through the air-fall tephra on Sólheimajökull (Fig. 7) depicting the 6 layers sampled.

Grain size distributions

There is significant variation between some of the layers in the air-fall tephra (Fig. 9). There is a particularly fine-grained layer in the middle of the deposit (layer C in Fig. 8) with 36% <63 µm. The top layer (F) is particularly course however, this is probably due to wind exposure blowing away the fines. The other 4 layers have largely similar grain size distributions, although the 2 layers beneath layer C do have a slightly higher percentage <63 µm (23%) compared to those above it (16%). At this stage it is hard to know whether the results represent different phases of the eruption, or whether the variation in grain size distributions is caused by a change in the predominant wind-direction.

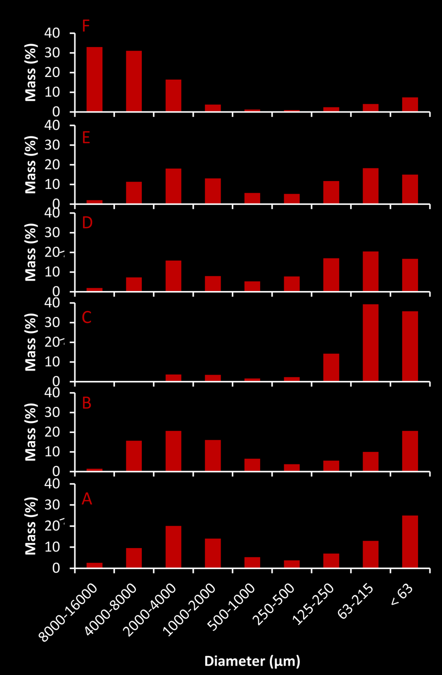

Figure 9: Grain size distributions for the 6 layers depicted in Figure 8.

FTIR

The air fall tephra has a matrix glass water content of ~0.1 wt.% consistent with degassing to atmospheric conditions. The jökulhlaup samples have water concentrations of ~0.2 to 0.3 wt.%. The elevated H_2O concentrations may be caused by loading from water (<130 m) and/or ice (<120 m; i.e. ~30% of the original ice thickness) or fragmentation within the conduit (~40 m depth) and/or post quenching hydration.

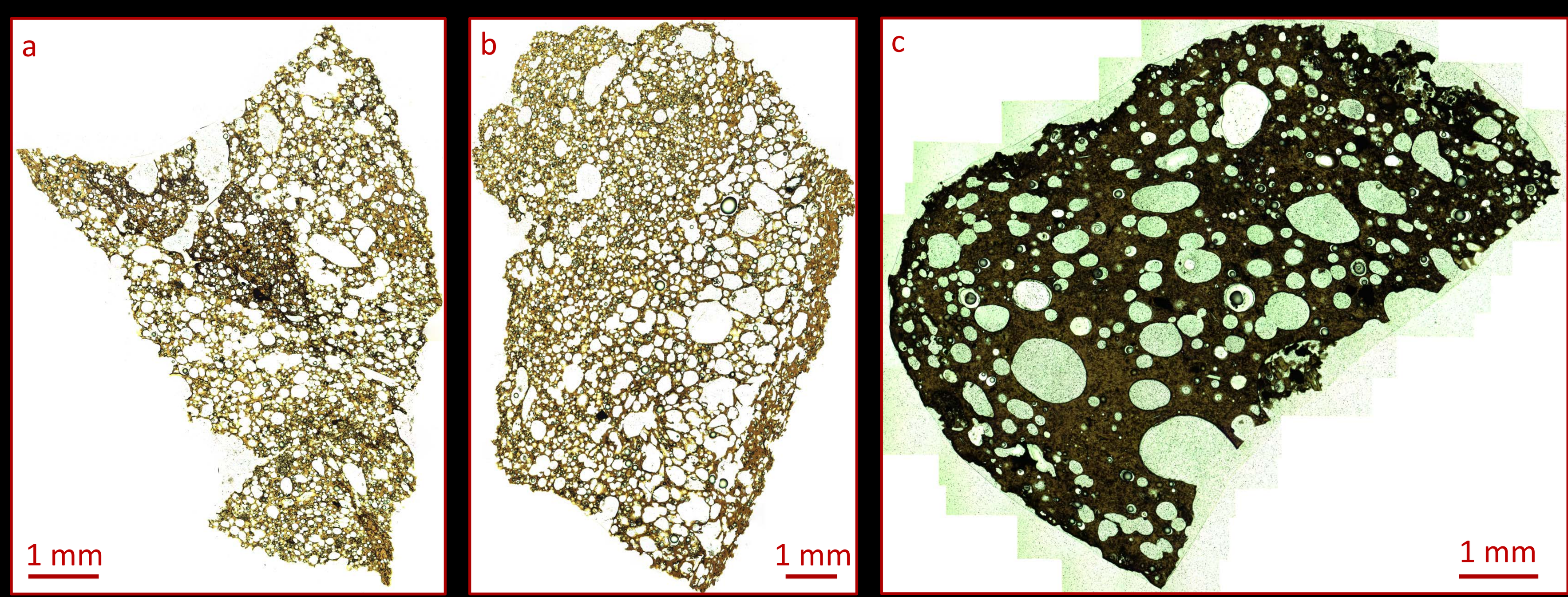

Figure 11: (a) A jökulhlaup clast showing evidence of clast welding; (b) A jökulhlaup clast showing bands of (left) small spherical bubbles, (middle) larger coalesced bubbles and (right) highly deformed bubbles; (c) A clast from the air-fall deposit; bubbles in the center of the clast appear larger than at the margins, perhaps as a result of continued bubble growth, post fragmentation.

TGA

Total volatile loss determined by weight change on heating, broadly agrees with the FTIR data (Fig. 10); clasts taken from the air-fall deposit have less total volatiles than those from the jökulhlaup deposits. It could be argued that within the jökulhlaup deposits, there is a slight decline of volatile concentrations with elevation, however, the difference is not significant enough to rule out natural variation and so more analyses are required.

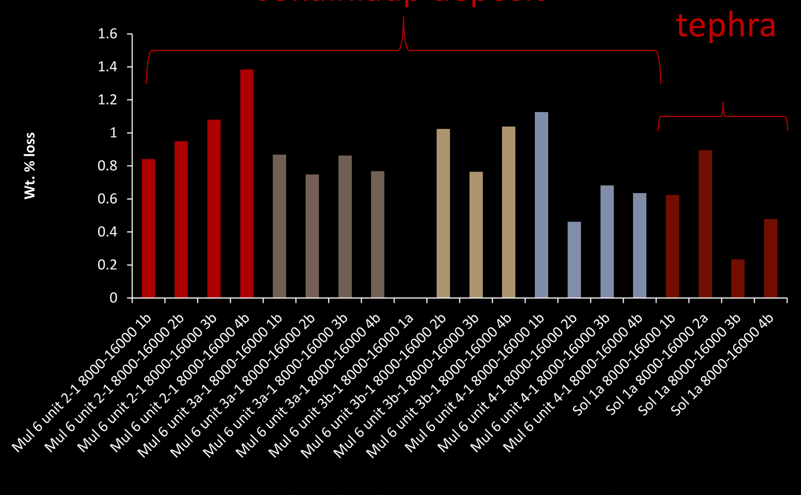

Figure 10: Total volatile loss determined using TGA. The units coincide with those labelled in Fig. 5

Textural analysis

All clasts have a high density of vesicles. However, the microlite content, bubble size and the degree of bubble deformation and coalescence all vary significantly (Figs. 11), suggesting that different clasts have been exposed to different degassing and cooling regimes. Some jökulhlaup clasts show evidence of clast welding (Fig. 11a) suggesting that quenching was not instantaneous and therefore fragmentation may have occurred within the conduit. The welding plus evidence of multiple phases of vesiculation could indicate that the magma has undergone multiple episodes of fragmentation and degassing.

Some clasts show strong heterogeneity in microlite content and/or bubble size/shape (Fig. 11b). This can be explained by localised sheer, clast welding and/or heterogeneous cooling. For example, some clasts appear to have an outer carapace of denser glass, with large bubbles in the clast core (Fig. 11c).

Hotstage

Bubble growth rates of ~1 µm s⁻¹ were determined using a hostage, for typical eruptive temperatures (Fig. 12). Based on a model for determining clast cooling rate within an aqueous setting[15], there would have been insufficient time to allow significant bubble growth within clasts that cooled in water. This agrees with bubble textures that show no significant spatial variation between the core and rim of the jökulhlaup clasts (Figs. 11a,11b). However, a clast from the air-fall tephra does show such variation (Fig. 11c). This suggests that in some cases, the clast interior stayed hot enough, for long enough, to allow continued degassing post-fragmentation and perhaps indicates that such clasts did not quench within water. This agrees with the inference based on the FTIR data that the air-fall tephra degassed under atmospheric conditions.

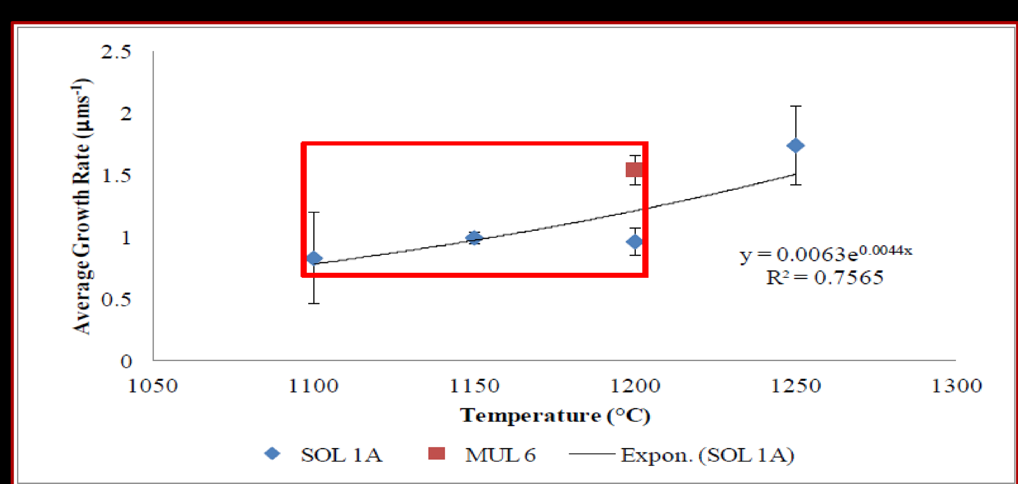

Figure 12: Bubble growth rates, determined using a hotstage, as a function of temperature. The red box represents the range of plausible Katla eruption temperatures . Sol 1a is an air-fall sample, Mul 6 was collected from the jökulhlaup deposits.

Conclusions

The data suggests that the air-fall tephra degassed under atmospheric conditions with little water interaction. By comparison the jökulhlaup samples seem to have quenched within water and under a slightly elevated pressure. Although, there is evidence of some post-fragmentation vesiculation, we believe that most degassing occurred in the conduit where there was probably repeated episodes of fragmentation and degassing.

Further work

Detailed SEM work of clast interiors to quantify the vesicle size distributions for the different clasts in the different units of the different deposit types.

An examination of the exterior clast morphologies to analyse whether fragmentation was dominated by vesiculation or magma-water interaction.

We will also look for differences in the volatile content, chemistry and textures of the clasts within the different units of the air-fall tephra, in order to try and explain the differences in grain size distributions. Do the different units represent different phases of eruptive behaviour and if so what was causing the change in eruption style?

References

1: Thorarinsson (1960) On the predicting of volcanic eruptions in Iceland, *B Volcanol,* 23(1): 45-52

2: Óladóttir et al., (2005) The Katla volcano S-Iceland: Holocene tephra stratigraphy and eruption frequency, *Jökull*, 55: 53-74

3: Icelandic Met Office: http://en.vedur.is/

4: Óladóttir et al., (2008) Katla volcano, Iceland: magma composition, dynamics and eruption frequency as recorded by Holocene tephra layers, *B Volcanol*, 70: 475-493

5: Cioni et al., (2014) Insights into the dynamics and evolution of the 2010 Eyjafjallajökull summit eruption (Iceland) provided by volcanic ash textures, *Earth Planet Sci Lett, 394: 11-123*

6: Owen et al., (2013a) Explosive subglacial rhyolitic eruptions in Iceland are fuelled by high magmatic H_2O and closed system degassing, *Geology*, *41*(2), 251-254

7: Guðmundsson et al., (2004) The 1996 eruption at Gjálp, Vatnajökull ice cap, Iceland: efficiency of heat transfer, ice deformation and subglacial water pressure , *B Volcanol, 66(1): 46-65*

8: Owen et al., (2013b) Pre-eruptive volatile content, degassing paths and depressurisation explaining the transition in style at the subglacial rhyolitic eruption of Dalakvísl, South Iceland, *J Volcanology Geoth Res*, *258*, 143-162.

9: O'Connor and Costa (2004) *The world's largest floods, past and present - their causes and magnitude*. US Geological Survey Circular 1254, 13p.

10: Tómasson (1996) The jökulhlaup from Katla in 1918, *Ann Glaciol*, *22*, 249-254

11: Larsen (2000) Holocene eruptions within the Katla volcanic system, south Iceland: Characteristics and environmental impact, *Jökull*, *49*, 1-28

12: Duller et al., (2008) Architectural analysis of a volcaniclastic jökulhlaup deposit, southern Iceland: sedimentary evidence for supercritical flow, *Sedimentology,* 55: 939-964

13: Jónsson (1980) Um Kötluhlaup, *Náttúrufræðingurinn,* 50(2): 81-86

14: Larsen (2010) Katla: tephrachronology and eruption history, *Dev Quaternary Sci,* 13: 23-49

15: Woodcock et al., (2012) Particle-water heat transfer during explosive volcanic eruptions, *J Geophys Res, 117(B10)*